JURNAL IPTEK
MEDIA KOMUNIKASI TEKNOLOGI
homepage URL : ejurnal.itats.ac.id/index.php/iptek

Numerical Investigation of Fluid in 2D and 3D Lid-Driven Cavity at Different Reynolds Numbers

Maria Margareta Zau Beu[1,3], Jiahn-Horng Chen[2]*

Program of Ocean Engineering and Technology, National Taiwan Ocean University, Keelung – Taiwan[1], Department of System Engineering and Naval Architecture, National Taiwan Ocean University, Keelung – Taiwan[2], Faculty of Mineral and Marine Technology - Institut Teknologi Adhi Tama Surabaya, Surabaya, Indonesia[3]

ARTICLE INFORMATION

Journal of Science and Technology – Volume 27 Number 1, May 2023

Page:
13 – 22
Date of issue :
May 30, 2023

DOI:
10.31284/j.iptek.2023.v27i1.3427

ABSTRACT

The lid-driven cavity (LDC), or cavity driven by a lid is a mechanical system that serves as a benchmark for studying various aspects of fluid mechanics. In this study, the incompressible fluid mechanics aspects were investigated using computational fluid dynamics (CFD) with a two-dimensional (2-D) and three-dimensional (3-D) LDC model. In the simulations, the lid moved unidirectionally along the x-axis, with Reynolds numbers $10 \leq Re \leq 35.000$. The flow simulations were performed in a steady state. The 2-D LDC simulations were conducted using mesh sizes of 501 × 501 and 601 × 601 grids, while the 3-D LDC model was simulated with a different grid size of 75 × 75 × 75. The flow patterns, velocity distributions, and vortex formation within the cavity were consistent with previous research findings and provided valuable insights into the understanding of flow behavior within enclosed cavities and the effects of lid movement on flow characteristics.

Keywords: *Lid-driven cavity (LDC), Reynolds number, CFD, Steady, Incompressible.*

E-MAIL

maria_margaret@itats.ac.id

PUBLISHER

LPPM- Adhi Tama Institute of Technology Surabaya
Address:
Jl. Arief Rachman Hakim No. 100, Surabaya 60117,
Tel/Fax: 031-5997244

ABSTRACT

Rongga yang digerakkan oleh tutup (Lid-driven cavity atau LDC) adalah sebuah sistem mekanik yang digunakan sebagai patokan untuk mempelajari berbagai aspek mekanika fluida. Dalam penelitian ini, aspek mekanika fluida tak termampatkan dipelajari menggunakan computational fluid dynamics (CFD) dengan model LDC dua dimensi (2-D) dan tiga dimensi (3-D). Dalam simulasi ini, tutup bergerak satu arah sejajar sumbu-x dengan rentang bilangan Reynolds antara $10 \leq Re \leq 35.000$. Simulasi aliran dilakukan dalam keadaan steady. Simulasi LDC 2-D menggunakan ukuran jaringan (mesh) 501 × 501 dan 601 × 601, sedangkan model LDC 3-D menggunakan ukuran jaringan berbeda, yaitu 75 × 75 × 75. Pola aliran, distribusi kecepatan, dan pembentukan pusaran (vortex) dalam rongga konsisten dengan temuan penelitian sebelumnya dan memberikan wawasan dalam memahami perilaku aliran dalam rongga tertutup serta efek gerakan tutup pada karakteristik aliran.

Kata kunci: *Lid-driven cavity (LDC), Reynolds number, CFD, Steady, aliran tak termampatkan.*

INTRODUCTION

The lid-driven cavity flow is primarily a research and benchmark problem in CFD, the insights gained from its study can be applied to certain industrial applications, particularly in areas such as automotive engineering, naval engineering, chemical processing, heat transfer systems, microfluidics, and optimization of industrial processes. The lid-driven cavity flow provides a simplified model for

understanding fluid behavior, its direct application to specific industrial problems requires additional considerations and modifications to account for the specific geometry, boundary conditions, and fluid properties relevant to the industrial process of interest.

Many researchers have shown their interest in studying flow problems in computational fluid dynamics (CFD) using the lid-driven cavity, starting with the early work of Burggraf [1]. Lid-driven cavities (LDCs) with internal flow type are of simple geometry, code and boundary conditions, etc. Although the problem looks simple in many respects, the flow in a cavity retains all the flow physics, with counter-rotating vortices occurring at the corners of the cavity. A comprehensive review of the subject was given by Erturk and Corke [2]. It was found that the Navier-Stokes equations in the flow function are solved numerically with a fine uniform grid of 601 × 601. The driven cavity flow was shown to have a quaternary vortex in the bottom left corner at a Reynolds number of 10,000 and a tertiary vortex in the upper left corner at a Reynolds number of 12,500. The boundary layer characteristics in the LDC flow can vary between two-dimensional (2D) and three-dimensional (3D) configurations [3]. In high Reynolds number flows, turbulence is a common phenomenon characterized by chaotic and unpredictable fluid motion. The importance of accurately resolving the turbulent flow in numerical simulations of confined volumes with high Reynolds numbers to obtain reliable and accurate results. However, simulating turbulence in confined volumes at high Reynolds numbers presents a number of challenges, such as grid resolution, boundary conditions, turbulence modeling, and simulation time. There is a need for research, which gives a brief overview of flow phenomena in a numerically simulated LDC with low to high Reynolds numbers.

The objective of this research is to examine the flow characteristics within an LDC in both 2D and 3D dimensions at various Reynolds numbers (ranging from 10 to 35,000) using CFD simulations. The simulations focus on achieving a steady-state condition, where the system or process remains constant over time. Steady-state simulations provide advantages such as computational efficiency, easier convergence, averaged results, and simplified interpretation, which makes them suitable for numerous CFD applications. However, the selection between steady-state and transient simulations should be based on the specific nature of the problem and the phenomena under investigation. The study presents detailed findings and includes comparisons with established benchmark solutions available in the literature.

LITERATURE REVIEW

The steady two-dimensional (2D) lid-driven cavity flow has been calculated using many different numerical methods. Benjamin and Denny have shown that when the Reynolds number is increased beyond Re = 1200, an additional secondary eddy occurs at the upper upstream corner [4]. Ghia has obtained highly-precision solutions using the coupled strongly implicit and multigrid methods with a grid as fine as 257 × 257 at Re = 7500 and 10,000, where two tertiary vortices appear in the corner regions [5]. Liao and Shu provide stability for viscous flows in driven cavities at high Reynolds numbers up to 10,000 [6]. Solutions for steady-driven cavity flow with Re values of 12,500 and 16,000 were provided by Barragy and Carey[7]. However, they found that the solution for Re = 16,000 exhibited oscillations related to boundary layer resolution problems due to the use of a coarse mesh. Steady solutions up to Re = 35,000 were reported by Wahba [8]. In their report, steady driven cavity flows up to Re = 35,000 are computed using a 501 × 501 grid and the results agree remarkably well with previous analytical solutions for driven cavity flows in the limit of infinite Reynolds number. For Re values up to 1000, all numerical studies in the literature report stable flow solutions. The agreement between these studies is also excellent, especially for the case Re = 1000. However, when the Reynolds number increases beyond 1000, the different studies tend to disagree. It is shown that driven cavity flows undergo supercritical *Hopf* bifurcation at high Reynolds numbers, leading to an unsteady flow. The term supercritical *Hopf* bifurcation generally refers to the local emergence of a periodic state from an equilibrium state when a certain parameter exceeds a critical value. In driven cavity flow, the critical parameter is the Reynolds number. This in turn means that the steady flow solution is no longer stable at high Reynolds numbers and therefore cannot be computed by numerical methods [9]. The *Hopf* bifurcation occurs at critical Reynolds numbers but is generally in the range of 7000 to 10,000 [10]. Some works address the question of whether it is possible to compute steady

solutions for driven cavity flows at *Re* values beyond the critical values. Examples of such studies include the work of Ghia et al.[5], which reports steady-state driven cavity flows up to *Re* = 10,000.

Moreover, Prasad and Koseff [11] have studied both experimentally and numerically the 3D flow in the LDC for Reynolds numbers in the range 1000 < *Re* < 10,000. They visualized the main circulation cell and the effect of increasing the Reynolds number by 10,000. These breakouts occur more frequently than at *Re* = 6000. The end walls also have a significant effect on the 3D flow. The end-wall vortices have a significant effect on the size of the downstream secondary vortex (DSV); as the span decreases, the size of the DSV decreases. Freitas et al. [12] have reported a 3D numerical simulation in the laminar flow regime where they reproduced the experimental results of the flow structure up to *Re* = 3200. The experimentally observed variation of the flow field structures over the span is reproduced by the simulated results. Energy from the velocity field changes the location and size of the vortex structures. Experimentally investigated the flow in a square cross-section cavity with dimensions 50.8 mm x 50.8 mm and with a span-wise aspect ratio (SAR) of 3:1 over a range of *Re* from 100 to 2000. Their study shows that the lid-driven cavity flow, which consists of primary and secondary vortices, changes from a local stable to a temporally periodic flow through a globally unstable condition, Aidun et al.[13].

METHODOLOGY

Physical Formulation

The schematic diagram of the LDC and the coordinate system is shown in Figure 1. The top wall of the cavity moves at a constant velocity. The fluid flow in LDC can be simulated by a set of mass and momentum conservation equations. The flow is assumed to be 2D and 3D, steady and incompressible. The governing equations for the incompressible steady-state flow can be described by the Navier-Stokes equations, which are a set of partial differential equations that govern fluid motion. For an incompressible flow, these equations can be written as follows:

continuity equation:

$$\nabla . u = 0 \quad \text{…. (1)}$$

momentum equations:

$$\rho(u.\nabla)u = -\nabla P + \mu\nabla^2 u \quad \text{…. (2)}$$

Here, $\boldsymbol{u}$ represents the velocity vector, P is the pressure, ρ is the fluid density, μ is the dynamic viscosity, and ∇ is the gradient operator. The continuity equation expresses the conservation of mass, stating that the divergence of the velocity vector field must be zero, indicating that the flow is incompressible. The momentum equations represent the conservation of momentum. The left-hand side represents the convective acceleration of the fluid, while the right-hand side accounts for the pressure gradient and the viscous forces. The pressure gradient (∇P) represents the force exerted by the pressure field, and the term $\mu\nabla^2\boldsymbol{u}$ represents the viscous forces, where μ is the dynamic viscosity and $\nabla^2\boldsymbol{u}$ is the Laplacian of the velocity vector.

Physical Model

Reynolds number, *Re*, is the ratio of inertial to viscous forces, that affects the flow properties within the cavity. The boundary condition of maintaining a constant velocity is imposed on all walls, excluding the upper lid. For the top lid or top wall moving in the positive *x*-direction, the velocity is $u = 1$; $v = 0$, and $z = 0$. All other lids or stationary walls are in no-slip condition, i.e., the fluid will have zero velocity relative to the boundary. The Velocity of the moving lid is equal to the length of the wall, where the dimension of the cavity wall is equal to one for the length (L), width (W), and height (H), the selection of this model is based on the literature from previous research, for 2D LDC [8] and 3D LDC [14]. The finite volume method is carried out using the commercial software ANSYS Fluent 19R1[15] to solve the governing equations under certain boundary conditions. The boundary conditions and dimensions of the computational domain are given in Table 1 and Table 2. A structured

grid fine mesh has been used, which gives a uniform grid in the core region and a denser grid near the cavity wall.

In this simulation, the quality of the mesh or grid is evaluated based on the aspect ratio of the mesh elements and the y^+ value. The aspect ratio represents the ratio between the longest and shortest sides of an element, while the y^+ value represents the dimensionless distance from the wall to the first grid point in the computational mesh, often the centroid of the nearest cell. The mesh used for numerical simulation consists of approximately 0.26 to 0.36 million cells with an aspect ratio of 1.2 for 2D models and 1.4 for 3D models. The y^+ value is used as a parameter to evaluate the ability of the mesh to accurately represent the boundary layer, and for both models, the y^+ value is less than one. Special attention was paid to fine-tuning the near-wall region to ensure accurate flow simulation in this region.

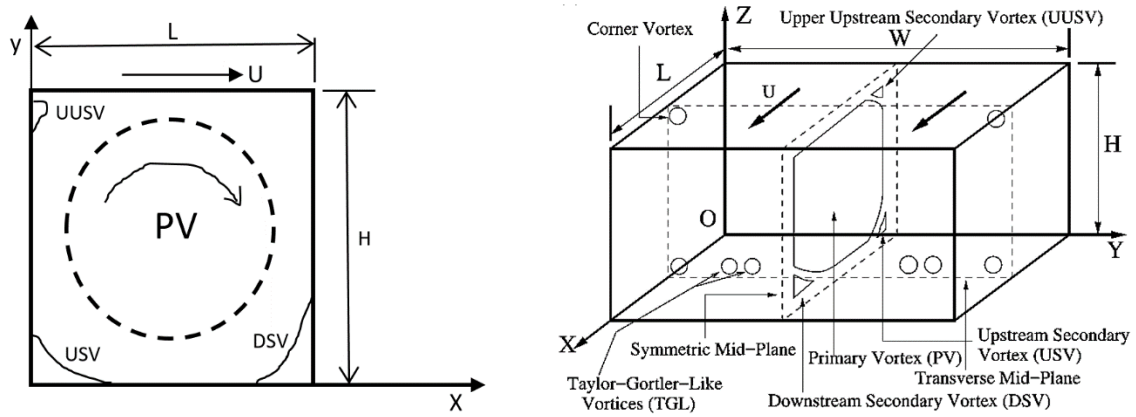

(a) (b)

Figure 1. Lid-driven cavity model (a) schematic of a 2D, (b) Schematic of a 3D[14].

Table 1. Boundary condition.

Geometry	For the top lid, z = H	
2D (Two dimensions)	x = L = u; $u=U_0$	Moving wall
	y = 0 and y = H	Stationary wall
3D (Three dimensions)	y = 0 and y = W	Stationary wall
	z = 0 and z = H	Stationary wall
No-slip condition		

Table 2. Domain and grid size.

Geometry of LDC	LDC size (L × W × H)	Grid number	Reynolds number (*Re*)
2D	1 × 1	501 × 501 601 × 601	*Re* = 10 *Re* = 1000 *Re* = 10,000 *Re* = 35,000
3D	1 × 1 × 1	75 × 75 × 75	

RESULTS AND DISCUSSION

The LDC numerical simulation 2D and 3D pressure-based solver with steady approach was applied. Spatial discretization was performed using the least square method. Each solution is allowed to go through 10,000 iterations to achieve the minimum convergence. Figure 2(a) and Figure 4(a) shown the average velocity on *x*-axis along the horizontal centerline (V_{avg}) of the cavity, while Figure 2(b) and Figure 4(b) shown the average velocity on *y*-axis along the vertical centerlines of the cavity (U_{avg}). The Reynolds number of 10 is simulated as a reference to observe the changes in the boundary layer as the Reynolds number increases. The average velocity on *x*-axis along the horizontal centerline (V_{avg}) of the cavity, as depicted in Figure 2(a) and Figure 4 (a) exhibit agreement with the experimental results of Erturk [2] and Ghia [5] for the 2D numerical simulations conducted with grid variations of

501 × 501 and 601 × 601, and *Re* = 1000. However, when the Reynolds number is increased to *Re* = 10,000 and 35,000, the agreement is observed between the research results and those of Wahba [8], as shown in Figure 2(a) and Figure 4(a). The Reynolds number is based on the maximum velocity of the lid (U_o) and the length of the cavity (L) and is defined as $Re = U_oL/\nu$, where ν is kinematic viscosity.

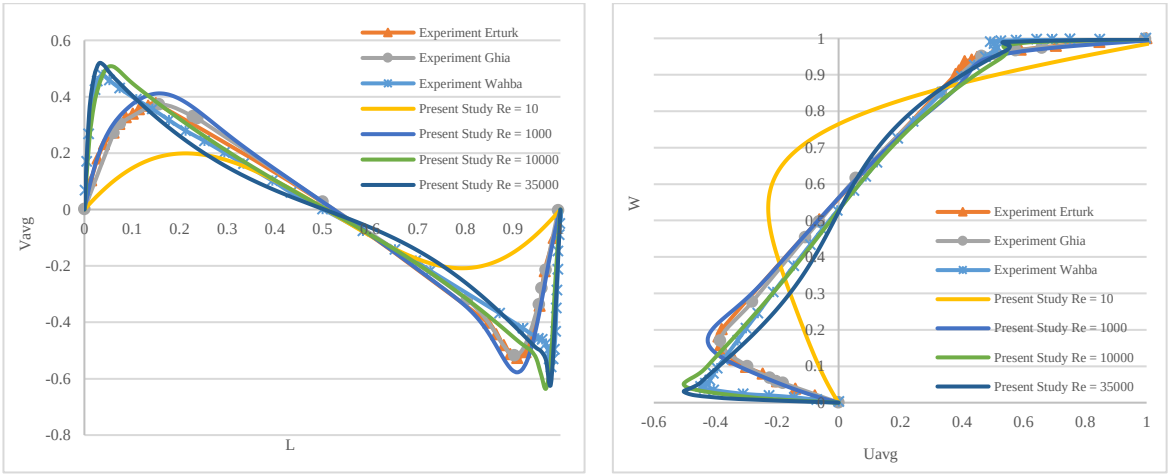

(a) (b)

Figure 2. Average velocity of 2D LDC using 501 × 501 grids; (a) the average velocity on *x*-axis along the horizontal centerline (V_{avg}); (b) the average velocity on *y*-axis along the vertical centerlines of the cavity (U_{avg}).

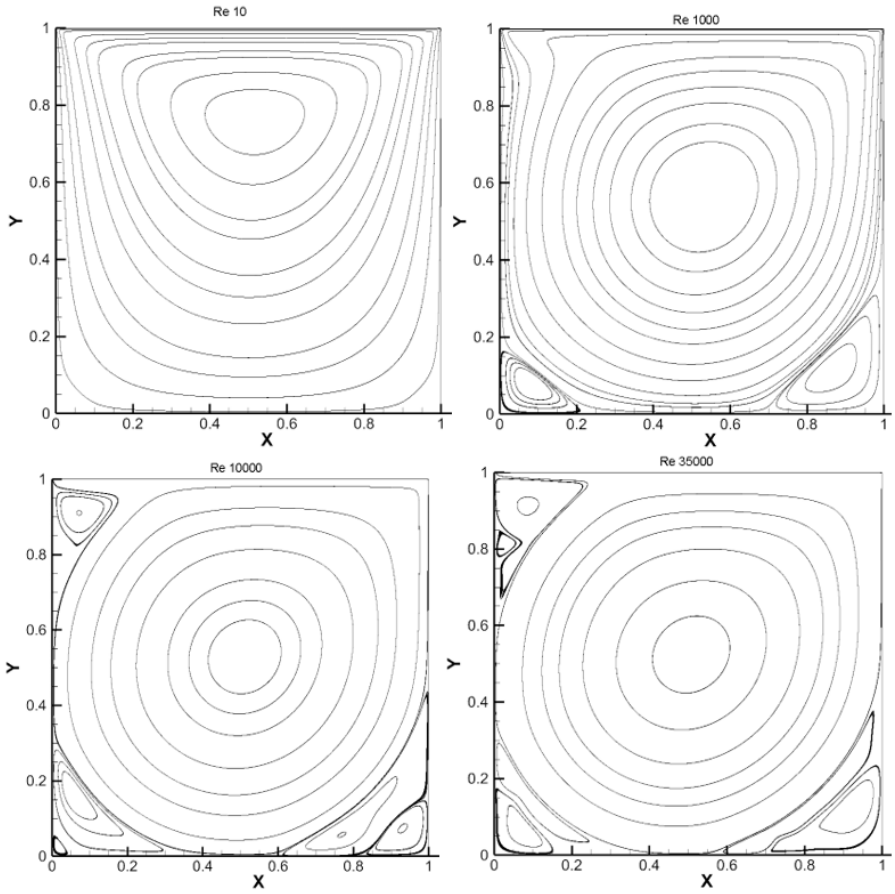

Figure 3. Streamlines velocity at different *Re* for 501 × 501 grid.

The average velocity on *y*-axis along the vertical centerlines of the cavity (U_{avg}), as depicted in Figure 2(b) and Figure 4 (b), exhibit agreement with the experimental results of Erturk[2] and Ghia

[5] for the 2D numerical simulations conducted with grid variations of 501 × 501 and 601 × 601, and *Re* = 1000. However, when the Reynolds number is increased to *Re* = 10,000 and 35,000, the agreement is observed between the research results and those of Wahba [8], as shown in Figure 2(b) and Figure 4(b). It can be observed that the velocity profiles become more sharply defined as the *Re* increases.

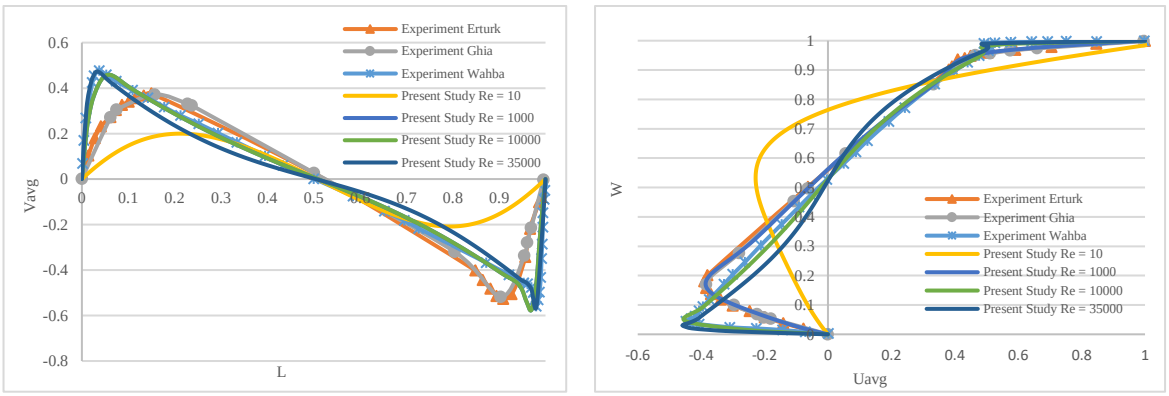

(a) (b)

Figure 4. Average velocity of 2D LDC using 601 x 601 grids; (a) the average velocity on *x*-axis along the horizontal centerline (V_{avg}); (b) the average velocity on *y*-axis along the vertical centerlines of the cavity (U_{avg}).

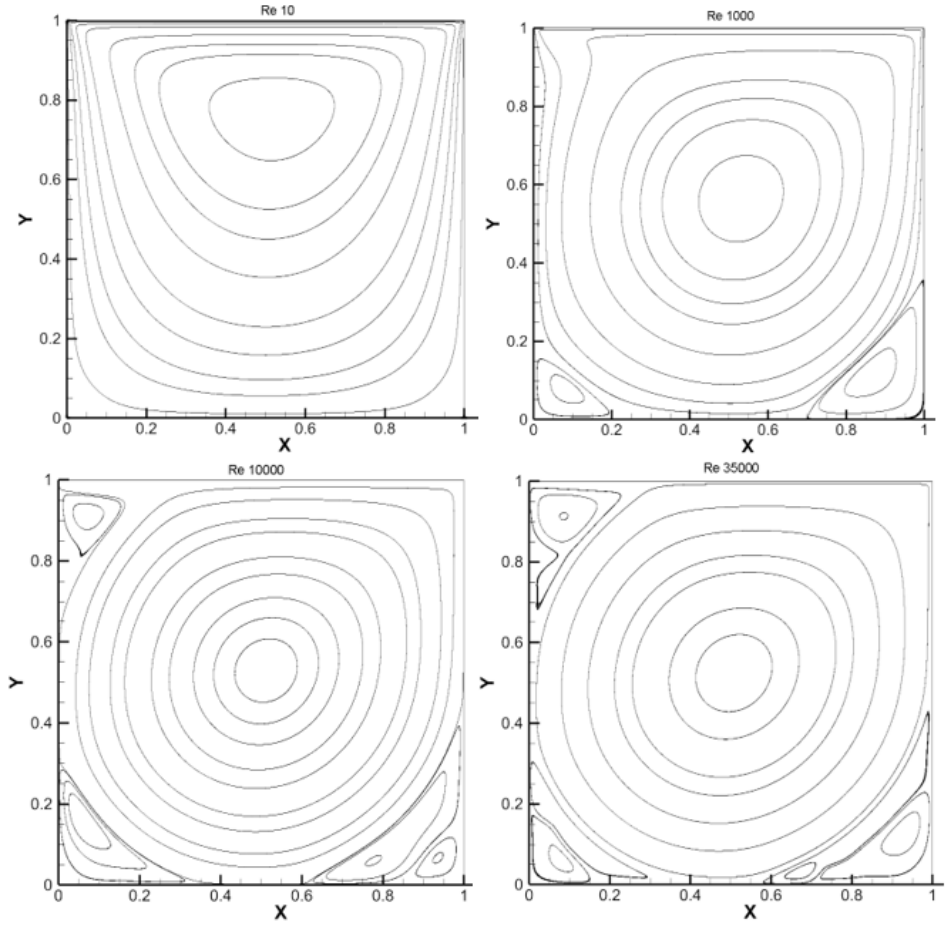

Figure 5. Streamlines velocity at different *Re* for 601 × 601 grid.

Figure 3 and Figure 5 depicted the streamlines and velocity contour, it shows the variations of the primary vortex (PV) with different grid configurations and Reynolds numbers. The characteristics of the primary vortex are summarized in Table 3. In flows *Re* = 10,000 and 35,000,

PV, USV and UUSV are generated, leading to an increased level of turbulence. The presence of these vortex influences the development of the boundary layer. The results obtained from the present scheme exhibit excellent agreement with the corresponding findings in the literature, as observed in the works of Wahba [8], these studies emphasize the increasing uniformity of the vorticity in the core of the LDC with increasing Reynolds number, indicating the thinning of the boundary layers at the stationary wall.

Table 3. The characteristics of the primary vortex (PV) at 2D LDC

Modeling	Grid number	*Re*	Location of the PV (*x*, *y*)
CFD	510 × 510	10	0.509; 0.769
		1000	0.518; 0.556
		10,000	0.513; 0.532
		35,000	0.493; 0.532
	601 × 601	10	0.518; 0.764
		1000	0.521; 0.561
		10,000	0.506; 0.529
		35,000	0.486; 0.529
Ghia [5]	257 × 257	1000	0.531; 0.562
		10,000	0.511; 0.533

In order to further investigation, the characteristics of the vortex in the LDC, a 3D flow simulation with grid sizes 75 × 75 × 75 and the y^+ values are also below one. The simulation results, as shown in Figure 6 and Figure 7 reveal the presence of the primary vortex (PV), downstream secondary vortex (DSV), upstream vortex (USV) at the symmetric middle plane (W/2) for *Re* = 1000. As the *Re* = 10,000, an additional vortex known as the upper upstream secondary vortex (UUSV) becomes apparent. This is consistent with the 2D LDC, where the UUSV becomes visible at *Re* = 10,000. Figure 8, for *Re* =1000, the average velocity has a higher value compared to *Re* =10,000 and 35,000. However, for *Re* =10,000 and 35,000, the average velocity profile exhibits sharper boundary layer profiles in the distribution of V_{avg} and W_{avg}. As the Reynolds number increases, the flow becomes more turbulent and chaotic. Turbulence enhances the mixing and diffusion of fluid particles, resulting in a thinner and more pronounced boundary layer.

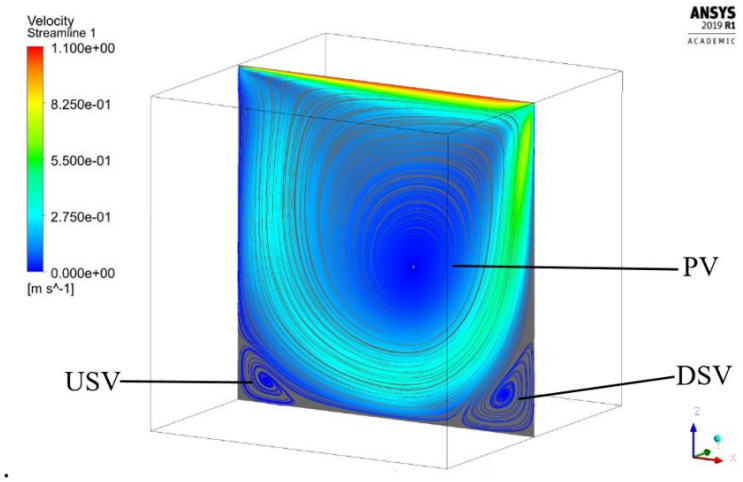

Figure 6. Streamlines velocity at the middle plane (W/2) of the cavity at *Re* = 1000

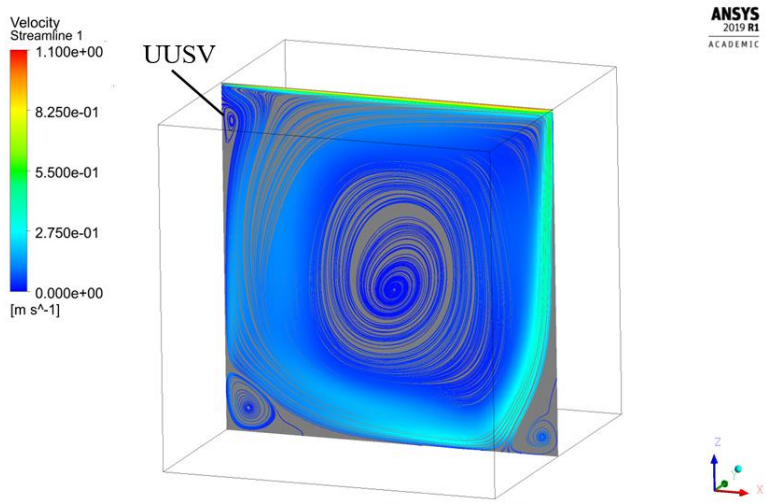

Figure 7. Streamlines velocity at the middle plane (W/2) of the cavity at *Re* = 10,000

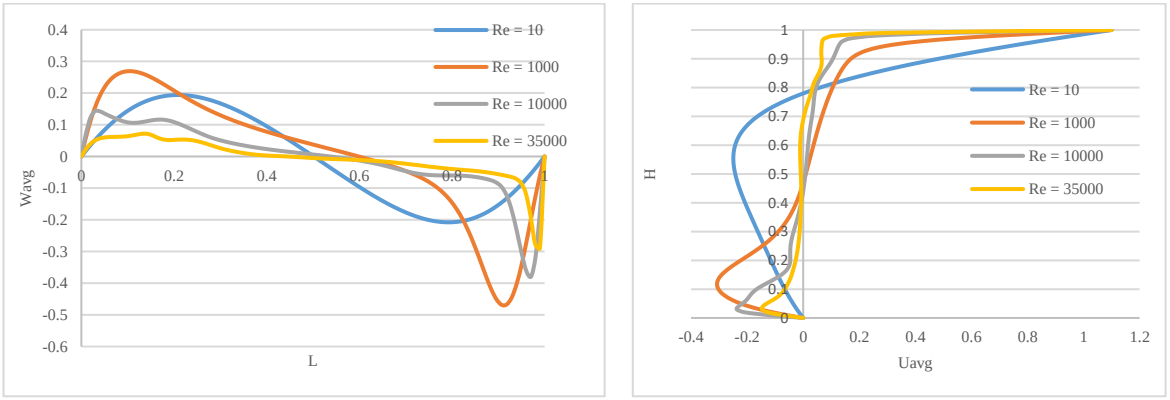

(a) (b)

Figure 8. Average velocity of 3D LDC in the mid-plane (W/2); (a) the average velocity on *x*-axis along the horizontal centerline (W_{avg}); (b) the average velocity on *z*-axis along the vertical centerlines of the cavity (U_{avg}).

CONCLUSIONS

The 2-D and 3-D lid-driven cavity (LDC) in steady-state solutions are computed for $10 \leq Re \leq 35{,}000$ with the 501 × 501 and 601 × 601 grids, respectively. For the 3D LDC model, the 75 × 75 × 75 grid was used. It was found that,

1. In 2D LDC simulation, the vortex such as DSV (downstream secondary vortex), USV (upstream secondary vortex) and UUSV (upper upstream secondary vortex) form at the corners of the cavity due to the no-slip condition at the walls and the increased *Re* value.
2. In 3D LDC simulations, similar to 2D LDC, the formation of vortex structures such as DSV, USV, and UUSV can occur. However, the presence and behavior of vortex such as DSV, USV, and UUSV can still affect the overall flow structure and lead to complex average velocity profiles due to the interaction between the vortices and the three-dimensional flow characteristics.
3. The Reynolds number (*Re*) significantly influences the flow development in a LDC, affecting vortex formation, flow recirculation, flow separation, and mixing characteristics. The transition from laminar to turbulent flow with increasing Reynolds number introduces additional complexity and alters the flow patterns and velocity profiles within the cavity.
4. In future CFD research and simulations, there are various factors that can affect the outcomes. These factors include the expertise and understanding of the user in CFD, the selection of physical models and assumptions, the quality of the grid or mesh used, the specification of boundary

conditions, the choice of turbulence modeling, the selection of numerical schemes and solvers, and the suitability of the computer specifications being used [16-18].

REFERENCES

1. Burggraf, O.R., *Analytical and numerical studies of the structure of steady separated flows.* Journal of Fluid Mechanics, 1966. 24(1): p. 113-151.
2. Erturk , E., Corke, T.C., *Numerical Solutions of 2-D Steady Incompressible Driven Cavity Flow at High Reynolds Numbers.* International Journal for Numerical Methods in Fluids, 2005: p. 747–774.
3. Erturk, E., *Discussions on driven cavity flow.* International Journal for Numerical Methods in Fluids, 2009. 60(3): p. 275-294.
4. Benjamin, A. and V.E. Denny, *On the Convergence of Numerical Solutions for 2-D Flows in a Cavity at Large Re.* Journal Of Computational Physics, 1979. 3: p. 340-358.
5. Ghia, U., Ghia, K.N., and Shin, C. T. , *High-Re Solutions for Incompressible Flow Using the Navier-Stokes Equations and a Multigrid Method.* Journal Of Computational Physics, 1982. 48: p. 387-411.
6. Liao SJ and J. Zhu, *A short note on higher-order stream function–vorticity formulation of 2-D steady state Navier–Stokes equations.* Int Journal for Numerical Methods in Fluids, 1996. 22: p. 1-9.
7. Barragy E and G.F. Carey, *Stream function–vorticity driven cavity solutions using p finite elements.* Computers & Fluids, 1997. 26(6): p. 453-468.
8. Wahba, E.M., *Steady flow simulations inside a driven cavity up to Reynolds number 35,000.* Computers & Fluids, 2012. 66: p. 85-97.
9. Wahba, E.M., *Multiplicity of states for two-sided and four-sided lid driven cavity flows.* Computers & Fluids, 2009. 38(2): p. 247-253.
10. Bruneau, C.H. and M. Saad, *The 2D lid-driven cavity problem revisited.* Computers & Fluids, 2006. 35(3): p. 326-348.
11. Koseff, J.R. and R.L. Street, *Visualization Studies of a Shear Driven Three-Dimensional Recirculating Flow.* J. Fluids Eng, 1984. 106: p. 21–27
12. Freitas, C.J., Street, R.L., Findikakis, A.N. and Koseff, J.R, *Numerical simulation of three-dimensional flow in a cavity.* International Journal for Numerical Methods in Fluids, 1985. 5: p. 561-575.
13. Aidun, C.K., N.G. Triantafillopoulos, and J.D. Benson, *Global stability of a lid-driven cavity with through flow : Flow visualization studies.* Phys. Fluids A, 1991. 3(9): p. 2081-2091.
14. Samantaray, D. and M.K. Das, *High Reynolds number incompressible turbulent flow inside a lid-driven cavity with multiple aspect ratios.* Physics of Fluids, 2018. 30(7).
15. Ansys., C., *Ansys fluent user guide.* 2015. Version 16.2.
16. Beu, M.M.Z. and J.-H. Chen, *Numerical Investigation of Incompressible Fluid In 3D Square Driven Cavity at High Reynolds Number.* 2021.
17. Beu, M.M.Z. and J.-H. Chen, *Assessment of subgrid-scale modeling for large-eddy simulation of lid-driven cavity SAR 0.5:1 incompressible turbulent flow.* 2021(Istanbul Technical University): p. 74-81.
18. Müller, J.-D., *Essentials of computational fluid dynamics*. 2015: CRC Press.

This Page Intentionally Left Blank